

See discussions, stats, and author profiles for this publication at: <https://www.researchgate.net/publication/321789294>

Using Sentinel-1 data for monitoring of soil moisture

Conference Paper · July 2017

DOI: 10.1109/IAGRSS.2017.8127291

CITATIONS

12

READS

1,723

3 authors:



Igor N. Garkusha

Dnipro Polytechnic National Technical University

12 PUBLICATIONS 30 CITATIONS

SEE PROFILE



Volodymyr Hnatushenko

Dnipro University of Technology

53 PUBLICATIONS 187 CITATIONS

SEE PROFILE



Volodymyr V. Vasyliiev

EOS DATA ANALYTICS, Inc.

22 PUBLICATIONS 154 CITATIONS

SEE PROFILE

Some of the authors of this publication are also working on these related projects:



influence of atmosphere and humidity [View project](#)



Pansharpening [View project](#)

USING SENTINEL-1 DATA FOR MONITORING OF SOIL MOISTURE

Igor N. Garkusha¹, Volodymyr V. Hnatushenko^{1,2}, Volodymyr V. Vasyliiev^{1,2}

¹ EOS Data Analytics Ukraine, Dnipro, Ukraine,

² Oles Honchar Dnipropetrovsk National University, Dnipro, Ukraine

ABSTRACT

Monitoring the soil moisture level of crop fields is one of the most important things to do for having an optimal crop yield. In this paper we investigate the capabilities of Sentinel-1 to soil moisture states. Aspects of modeling the map of soil moisture by the radar scene from Sentinel-1 on the example of a territory having undergone intensive precipitation have been considered. Representations of the territory with the radar and multispectral imaging are compared. Besides the meteorological satellite images and data of weather stations, additional verifying multispectral space images from Landsat-8 and Sentinel-2A were used. With the use of the obtained empirical model it became possible to build maps of soil moisture of the research territory for different times.

Index Terms—Radar imaging, Sentinel-1, soil moisture, polarization, amplitude

1. INTRODUCTION

With the launch of Sentinel-1, the European Space Agency (ESA) active radar satellites, in 2015-2-16, the interest to the results of processing radar data has increased. First of all, this was caused by public availability of level 1 preprocessing products: Single Look Complex (SLC) and Ground Range Detected (GRD), obtained from the satellites of this series. The SLC product containing the amplitude and phase components of the radar signal is used for plotting interferograms and maps of dislocations of the Earth's surface. The GRD product contains only the amplitude component of the radar signal and can be used in solving a wide range of problems of the Earth surface monitoring, for instance, problems of the agroindustrial complex, forestry and others.

However, there are a number of essential issues that researchers should take into account while processing radar imagery data. For instance, research of a number of experts in this field [1–3] has shown that the atmosphere of the Earth influences the radar imagery data as well. Moreover, there are existing ready products of radar data processing, featuring information, for instance, on wind speed,

atmospheric conditions and rain fronts [1, 2, 4]. Troposphere and ionosphere influence the phase of the radar signal causing delays. Besides, as observations over the amplitude of radar signals have shown, weather conditions also influence it [1]. Therefore, taking into account the increasing role of radar imaging, research in this direction is topical. The main goal of this work was to study the influence of the atmosphere and humidity of the air on the quality of representation of an imagery territory with the GRD products.

2. STUDY AREA AND SOURCE DATA

Fig. 1 shows a research territory – an area comprising the mouth of the Dnipro River and a part of the north-west coast of the Black Sea (the area of the observation territory is around 44 790 km²). As the initial data, five GRDH (GRD High Resolution, the spatial resolution in such product is around 10 m) products were taken. Dates of taking: 06.09.2016, 18.09.2016, 30.09.2016, 12.10.2016, 05.11.2016.

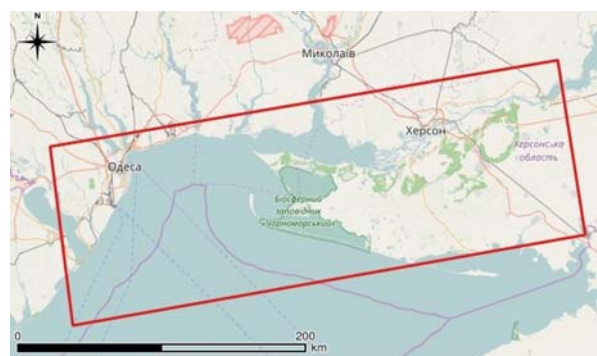


Fig.1. The territory of research

Basing on the dates of imaging, for the chosen research territory we made a search for scenes, which would allow us to evaluate presence of cloudiness and atmospheric influence. Such scenes were space images from remote sensing satellite Terra/Aqua and products of visualization of Multi-Sensor Precipitation Estimate (MPE) by the European organization EUMETSAT, which were obtained via the LightningMaps internet resource (www.lightningmaps.org).

Also information on weather conditions from the weather station of the city of Odessa and weather archives of the weather on the cities of Nikolayev and Kherson – the nearby big cities on the research territory – was used.

The archive data confirms stable dry weather at the moment of imaging by Sentinel-1 on 30.09.2016 and very rainy weather at the moment of imaging on 12.10.2016. Besides the meteorological satellite images and data of weather stations, additional verifying multispectral space images from Landsat-8 and Sentinel-2A were used.

3. DATA PROCESSING

The five selected products of processing Level-1 C Sentinel-1 GRDH are represented by amplitude values of signals of two polarizations, VV and VH. Each polarization channel of a particular scene underwent preprocessing operations:

- Use of the Orbit File data for more accurate operations of geocoding of the image.
- Calibration of the channel data with the purpose of obtaining the values of the radar backscatter coefficient σ^0 .
- Speckle filtering.
- Geocoding of the processed scenes with the use of the Digital Elevation Model (DEM).
- Conversion of σ^0 values into the scale of dB units recommended for analysis of this kind.

All operations were performed in the automated mode with the use of EOS DA SAR Processing Toolbox developed on the base of radar data processing library ESA SNAP. For visualization in the research, software product Quantum GIS (QGIS) was chosen.

In color RGB-synthesis of radar data, one can use either calibrated values σ^0 of respective polarizations or their combinations. For instance, ratio: $\sigma_{VV}^0 / \sigma_{VH}^0$. Thus, the processed scenes are represented in the RGB-synthesis by data channels: $\sigma_{VV}^0 - \sigma_{VH}^0 - \sigma_{VV}^0 / \sigma_{VH}^0$. For instance, in Fig. 2 and Fig. 3, colored synthesized images of the scenes dated 30.09.2016 and 12.10.2016 are presented. All five radar scenes were performed from the same track and with almost the same incidence angle of the radar beam – from 30.2° to 45.8° .

4. RESULTS AND DISCUSSIONS

In the visualized scenes it is immediately obvious that they have substantial color differences, that is, are substantially different in values in the respective channels of the RGB synthesis. For further and more detailed analysis, a test part with the area of 250 km^2 was selected (Fig. 4).

It is known that the intensity of reflection of the radar signal depends on several factors [5, 6], one of which is dielectric permittivity of a material. At that, one should

remember that dielectric properties of materials are influenced by moisture and temperature. With the growth of moisture, dielectric properties of objects on the surface of the earth will deteriorate. One also has to remember that for different materials, dielectric permittivity will change with the change of the frequency of the signal. A good example of change of dielectric properties is water – the value of its permittivity changes with the change of both frequency of the signal and the temperature. As it was mentioned above, on 12.10.2016 intensive precipitations were registered on the research territory. Mainly, exactly the change of moisture of soil explains the color difference in the presented images.

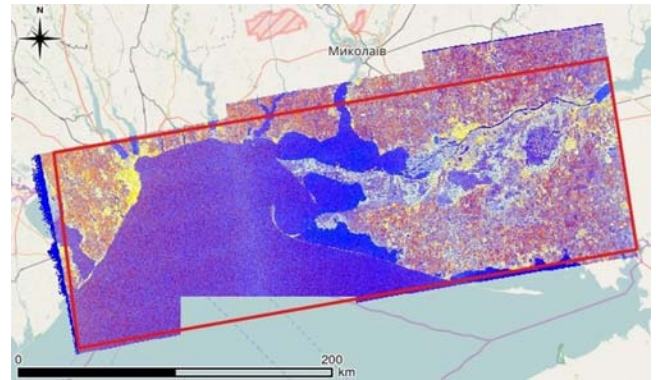


Fig.2. A radar image of the research territory – calibrated product of processing from Sentinel-1A GRDH. RGB synthesis: $\sigma_{VV}^0 - \sigma_{VH}^0 - \sigma_{VV}^0 / \sigma_{VH}^0$. Date of taking: 30.09.2016

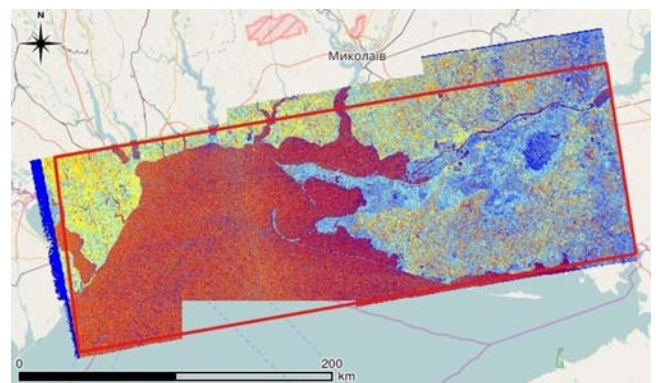


Fig.3. A radar image of the research territory – calibrated product of processing from Sentinel-1A GRDH. RGB synthesis: $\sigma_{VV}^0 - \sigma_{VH}^0 - \sigma_{VV}^0 / \sigma_{VH}^0$. Date of taking: 12.10.2016



Fig.4. The test part of the research territory. Area: 250 km^2

Figs. 5 and 6 show comparisons of fragments of radar scenes with the high resolution multispectral images from Sentinel-2A and Landsat-8.

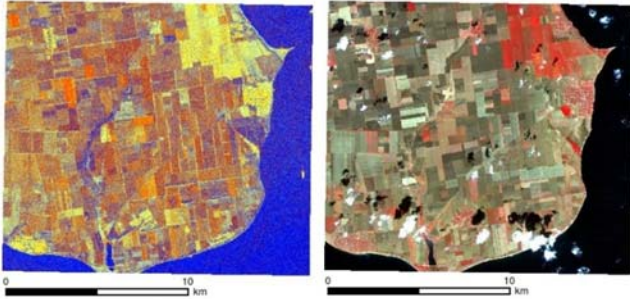


Fig.5. A fragment of a radar image of the test part of the research territory (left) and a fragment of color synthesized multispectral image (channels 8-4-2) from Sentinel-2A (right). Dates: 30.09.2016 (left), 22.09.2016 (right)

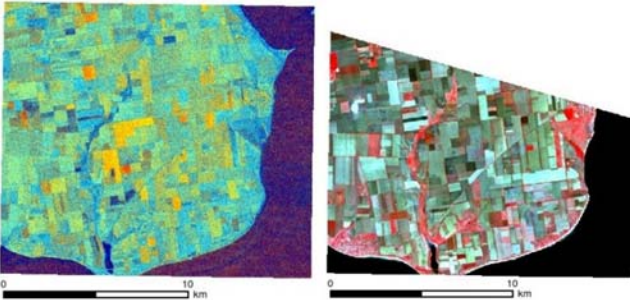


Fig.6. A fragment of a radar image of the test part of the research territory (left) and a fragment of color synthesized multispectral image (channels 5-4-2) from Landsat-8 (right). Dates of taking: 12.10.2016 (left), 10.10.2016 (right)

In Fig. 5 is clearly seen that in the color synthesis of channels 8-4-2 (near infrared - red - light blue) of Sentinel-2A's MSI scanner, fields rendered in bright red colors (located in the upper right corner of the image) have well-developed vegetation. In Fig. 5, these fields are represented by shades of yellow. As it is seen from comparing the scenes, water is of blue color, and the exposed soil of fields, of brown and red shades. Red and orange are fields with short vegetation, presented in the multispectral image with light gray hues. Small settlements located by the Black sea shore have good vegetation, and for this reason, in the radar scene they are also shown in hues of yellow. The dampened river banks, as well as some fields saturated with moisture and areas of the wet coastal zone, are also colored in blue tones.

As it is seen in Fig. 6, the Landsat-8 image partially covered the territory of interest, but even in it, changes in the vegetation composition of the territory are clearly seen. Thus, it is seen that the river banks, because of good moistening, become covered with green vegetation. Well-moistened field and coastal areas on the right of the image

are also covered with greenery. However, in Fig. 6 (left, radar image) this is not visible – these areas are shown only in blue hues. The color of the water surface is also distorted and has a tinge of red hues. This is particularly clearly seen in Fig. 3, covering the whole scene of the research territory. In general, colors are not the same as in Fig. 5. The scene from Sentinel-2A of this territory dated 12.10.2016 is completely covered with dense clouds. Thus, one can conclude that indeed, even in the case of dense and thick cloudiness, users will obtain an image of a radar scene from Sentinel-1, but they will encounter a problem of interpreting objects on the territory owing to increased moisture, if such will be caused by atmospheric precipitations. Besides, an excessively moistened scene contains more noise.

In [6] it is shown that the value of the σ^0 coefficient is well-agreed with such property as moisture of soil, and such dependence is linear. For a more accurate determination of correlation between the moisture of soil and values of the σ^0 coefficient, data collected from specialized weather stations of the observation network U.S. Climate Reference Network (USCRN) were used. Also, data of products Sentinel-1A GRDH were used.

Table 1 represents values of the key parameters measured by one of the CRN stations (USCRN Chillicothe – Latitude: 39.87°, Longitude: -93.15°), and values σ_{VV}^0 and σ_{VH}^0 . The value of averaged per hour volumetric water content of the soil θ is presented by the ratio of the volume of water to the volume of soil (m^3 of water/ m^3 of soil) by the data of five-minute measurements during an hour, obtained from sensor at the depth of 5 cm. In the table also presented average relative humidity of the air (RH) and the temperature on the surface of soil (T_{LST}). Comparison of the data of the VV polarization channel and moisture of the soil is presented in Fig. 7.

Scaling was done with the use of the following expressions:

$$\sigma_{VV'}^0 = 5 \cdot \sigma_{VV}^0 + 100; \quad \theta' = \theta \cdot 100.$$

Table 1. Values of the parameters from the weather station and values of the σ^0 coefficient

Date of measurement by the CRN-station	σ_{VV}^0 , dB	T_{LST} , °C	RH, %	θ (depth 5 cm), m^3/m^3	$\theta \times 100$ (depth 5 cm), m^3/m^3	$\sigma_{VV'}^0$, dB
09.01.2016	-9.98	+2.2	94	0.54	54.3	50.12
21.01.2016	-16.56	-11.9	81	0.35	34.7	17.23
08.05.2016	-13.27	+17.7	63	0.33	33.2	33.65
13.06.2016	-13.96	+27.8	52	0.25	25.0	30.22
07.07.2016	-7.52	+25.9	79	0.53	52.6	62.40
31.07.2016	-7.56	+24.9	62	0.21	21.1	62.21

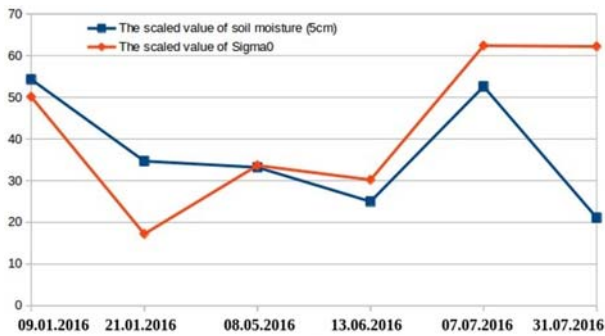


Fig.7. Correlation of the scale-adjusted values of the soil moisture and the σ_{VV}^0 coefficient

In Fig. 7 it is seen that the values of the scaled σ_{VV}^0 are sufficiently close to the values of θ' for all days, except 21.01.2016 and 31.07.2016. According to the weather station, on 21.01.2016 low temperature and high humidity was registered, but the soil at the depth of 5cm was not very humid. On 31.07.2017, at a relatively high humidity, moisture of the soil at the depth of 5cm was low.

In different studies it was pointed out that, since soils may substantially vary in composition, salinity and their chemical components, it is rather difficult to work out a universal mathematical model of transition from values σ^0 of the polarization data of active radar systems to θ , however, approximate models do exist [5, 6].

The proposed in the research linear model for translation of values makes it possible to approach the existing θ values with the error 0.058 by using the following expression for obtaining the model value of θ' :

$$\theta' = 0.05 \cdot \sigma_{VV}^0 + 1 ; \text{ if } \theta' < 0 \text{ then } \theta' = 0.$$

5. CONCLUSION

Thus, with the use of the obtained empirical model it became possible to build maps of moisture of the research territory for different times (Figs. 8 and 9).

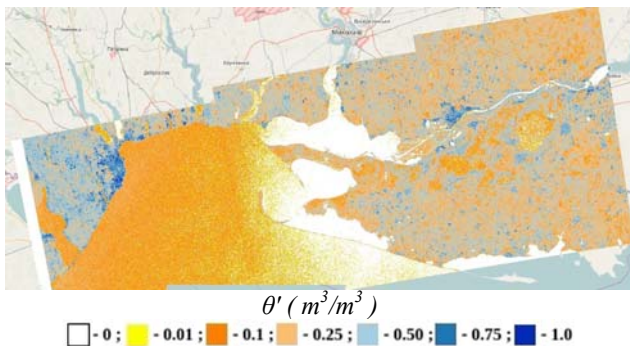


Fig.8. A modeled map of moisture of soils on 30.09.2016

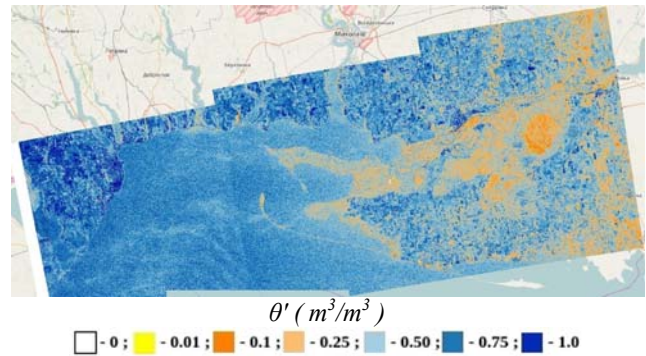


Fig.9. A modeled map of moisture of soils on 12.10.2016

Fig. 8 shows water surface incorrectly. In Fig. 9 excessively moistened parts of land are clearly highlighted, especially near the city of Odessa, where the precipitation was considerable and where, according to the weather station, the relative humidity of 100% was observed. The least moistened area is the Oleshkiv Desert about the city of Kherson.

Further development of this research is planned to be devoted to obtaining maps of soil moisture of higher reliability, as well as the research of the possibility of working out a mathematical model linking the indicator of soil moisture with vegetation indexes obtained from the multispectral imaging data.

6. REFERENCES

- [1] C. R. Jackson, J. R. Apel, "Synthetic Aperture Radar Marine User's Manual". U.S. Department of Commerce, 2005.
- [2] "Guide to Meteorological Instruments and Methods of Observation" Geneva, Switzerland: World Meteorological Organization, 2010. Print.
- [3] A. Akkartal A and F. Sunar A., "The usage of radar images in oil spill detection", *The international archives of the photogrammetry, remote sensing and spatial information sciences*, vol. XXXVII, part B8, Beijing, 2008, pp. 271-276.
- [4] S. Lehner, B.Tings, "Maritime products using Terrasar-X and Sentinel-1 imagery", 36th International Symposium on Remote Sensing of Environment, 11–15 May 2015, Berlin, Germany, 2015, pp. 967-973.
- [5] Tarendra Lakhankar and Nir Krakauer and Reza Khanbilvardi, "Applications of microwave remote sensing of soil moisture for agricultural applications" *Int. Journal Terraspace Sci. Eng.*, 2009, pp. 81–91.
- [6] M. Zribi, N. Baghdadi, N. Holah, O. Fafin, "New methodology for soil surface moisture estimation and its application to ENVISAT-ASAR multi-incidence data inversion", *Remote Sensing of Environment*, 96, 2005, pp. 485-496.